JASEM ISSN 1119-8362

Full-text Available Online at
https://www.ajol.info/index.php/jasem
http://ww.bioline.org.br/ja

J. Appl. Sci. Environ. Manage.
Vol. 22 (4) 499 – 502 April 2018

Crack Growth Analysis in Aluminium Alloy Plate (Al 2024 - T351) Using Finite Element Method

[1*]ERHUNMWUN, ID; [1]IKPOZA, E; [2]IKPONMWOSA, UB

[1]Department of Production Engineering, [2]Department of Petroleum Engineering, University of Benin, Benin City, Nigeria.
**Corresponding E-mail: iredia.erhunmwun@uniben.edu*

ABSTRACT: In this paper, an aluminium alloy (Al 2024 – T351) was discretized into four linear elements and crack growth rate analysis was carried out using the Finite Element Method (FEM). The overall results from these finite elements were finally assembled to represent the crack growth in the entire domain of the aluminium alloy. The results obtained from the finite element method shows that as the number of cycle increases, the crack growth also increases linearly. This was shown for different cycle from 0 to 4000 with an initial crack growth of 0.05mm. The result obtained from the FEM when compared with the result obtained from the exact differential equation method shows a strong agreement.

DOI: https://dx.doi.org/10.4314/jasem.v22i4.10

Dates: Received: 19 March 2018; Revised: 10 April: 2018; Accepted: 19 April 2018

Keywords: Crack, Priddle Model, Weak Formulation, Aluminium Alloy.

Surface cracks, which are most likely to be found in many structures in service, such as Pressure vessels, pipeline systems, is recognized as a major origin of potential failure for such components. The study of fatigue crack propagation from such defects has been an important subject during recent decades. The first fatigue crack propagation expression formulated in terms of the stress intensity factor was proposed by Paris et al. (1963). The relation states that in the log-log scale the fatigue crack growth rate (FCGr), $\frac{da}{dN}$ depends linearly on the applied stress intensity factor range, ΔK_{appl} in the region II of fatigue rate curve. Walker (1970) proposed a model to improve the Paris model by including three curve fitting constant, C, m and γ. Forman (1972), proposed a relation that explain the stress ratio effect on FCGr which is also effective in Region III of fatigue growth curve using fracture toughness, K_c and two curve fitting constants C and m. Broek (1989), Schijve (1999), and Erdogan proposed a relation, which accounts for the mean stress effect in region II of fatigue rate curve (Broek, 1989) with C as only curve fitting constants. Weertman model is applicable only in regions II and III (intermediate and high propagation rate) of fatigue rate curve and it uses only one curve fitting constant. (Weertman, 1966). McEvily (1979) proposed another empirical relation based on the same logic as Priddle's relation and which could describe the entire fatigue crack growth curve. Collipriest (1972) proposed a crack growth model capable of describing all three regions of fatigue rate curve and includes the stress ratio effect. Priddle (1995) proposed the equation which can describe the fatigue rate curve in all three regimes by introducing fracture toughness, K_c and threshold stress intensity range, ΔK_{th} in the fatigue growth model. The Priddle's relation, eq. 1, is based on two assumptions. The model requires the prior knowledge of two material constants, ΔK_{th} and K_c, and two additional curve fitting constants C and m which are curve fitting constants. This work present the analysis of crack growth in an aluminium alloy using the Priddle model.

MATERIALS AND METHOD

Governing Equation: The Priddle model is given as:

$$\frac{\partial a}{\partial N} = C\left(\frac{\Delta K_{appl} - \Delta K_{th}}{K_{IC} - K_{\max}}\right)^m \text{ (Priddle, 1995)} \qquad 1$$

Where
$a =$ Crack Length, N= Number of Cycle,
$\Delta K_{appl} =$ Applied Stress Intensity Factor,
$\Delta K_{th} =$ Threshold Stress Intensity Range,
$K_{IC} =$ Plane Strain Fracture Toughness ,
$K_{\max} =$ Maximum Stress Intensity Factor,
C and m are curve fitting constants.

**Corresponding E-mail: iredia.erhunmwun@uniben.edu*

Let $y = C\left(\frac{\Delta K_{appl} - \Delta K_{th}}{K_{IC} - K_{max}}\right)^m$ 2

Eq. 1 becomes

$$\frac{\partial a}{\partial N} - y = 0 \quad 3$$

Weak Formulation: In the development of the weak form, we assumed a linear mesh and placed it over the domain and applied the following steps:

Multiply eq. 3 by the weighted function (w) and integrate the final equation over the domain.

$$\int_{N_A}^{N_B} w \frac{\partial a}{\partial N} dN - y \int_{N_A}^{N_B} w dN = 0 \quad 4$$

*Interpolation Function***:** The weak form in eq. 4 requires that the approximation chosen for 'a' should be at least linear in 'N' so that there are no terms in eq. 4 that are identically zero. We proposed that 'a' is the approximation over a typical finite element domain by the expression:

Let $w = \psi_i$ and $a = \sum_{j=1}^{n} a_j \psi_j$ 5

Substitute eq. 5 into eq. 4

$$\sum_{j=1}^{n} a_j \int_{N_A}^{N_B} \psi_i \frac{\partial \psi_j}{\partial N} dN - y \int_{N_A}^{N_B} \psi_i dN = 0 \quad 6$$

In matrix form,

$$\lfloor K_{ij} \rfloor a_j - y\{f_i\} = 0 \quad 7$$

where $K_{ij} = \int_{N_A}^{N_B} \psi_i \frac{\partial \psi_j}{\partial N} dN$ and $f_i = \int_{N_A}^{N_B} \psi_i dN$ 8

The interpolation function used is a linear, one dimensional function as in eqs. 9 and 10.

$$\psi_1 = 1 - \frac{N}{h} \quad 9$$

$$\psi_2 = \frac{N}{h} \quad 10$$

Analysis of the $\lfloor K_{ij} \rfloor$ Matrix

In matrix form, we have;

$$[K_{ij}] = \begin{bmatrix} \frac{N_A}{h} - \frac{1}{2} & -\frac{N_A}{h} + \frac{1}{2} \\ -\frac{N_A}{h} - \frac{1}{2} & \frac{N_A}{h} + \frac{1}{2} \end{bmatrix} \quad 11$$

Assembly of the $[K]$ matrix gives

$$[K_{ij}] = \frac{1}{2}\begin{bmatrix} -1 & 1 & 0 & 0 & 0 \\ -1 & 2 & -1 & 0 & 0 \\ 0 & -3 & 6 & -3 & 0 \\ 0 & 0 & -5 & 10 & -5 \\ 0 & 0 & 0 & -7 & 7 \end{bmatrix} \quad 12$$

Analysis of the $\{f_i\}$ Matrix

In matrix form, we have:

$$\{f_i\} = \begin{Bmatrix} -N_A + \frac{h}{2} \\ N_A + \frac{h}{2} \end{Bmatrix} \quad 13$$

Assembly of the $\{f_i\}$ matrix gives

$$\{f_i\} = \frac{h}{2}\begin{Bmatrix} 1 \\ 0 \\ 0 \\ 0 \\ 7 \end{Bmatrix} \quad 14$$

Substitute eqs. 12 and 14 into eq. 7, we have:

$$\begin{bmatrix} -1 & 1 & 0 & 0 & 0 \\ -1 & 2 & -1 & 0 & 0 \\ 0 & -3 & 6 & -3 & 0 \\ 0 & 0 & -5 & 10 & -5 \\ 0 & 0 & 0 & -7 & 7 \end{bmatrix}\begin{Bmatrix} a_1 \\ a_2 \\ a_3 \\ a_4 \\ a_5 \end{Bmatrix} = hy\begin{Bmatrix} 1 \\ 0 \\ 0 \\ 0 \\ 7 \end{Bmatrix} \quad 15$$

RESULTS AND DISCUSSION

The data given below are for Al 2024 - T351

$C = 2.606 \times 10^{-4}$, $m = 1.102$; $-2 < R < 1$ (Abhishek et. al., 2013)

$\Delta K_{th} = 2.2MPa\sqrt{m}$; $K_{IC} = 34.1MPa\sqrt{m}$; $K_{max} = 30\,MPa\sqrt{m}$

Substituting these parameters into eq. 2, we have

$$y = 5.5041 \times 10^{-5} \times (\Delta K_{appl} - 2.2)^{1.102} \quad 16$$

The initial crack $(a_o) = 0.05mm$ and $\Delta K_{appl} = 3.5MPa\sqrt{m}$

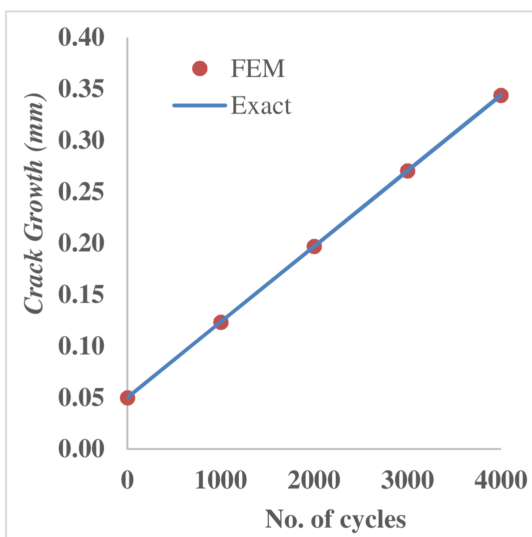

Fig. 1: Crack Length against No. of Cycles

The exact differential equation solution of the Priddle model is shown in eq. 17.

$$a_{i+1} = a_0 + y\left(N_{i+1} - N_i\right) \quad 17$$

Where $a_0 =$ Initial Crack Length

Table 1: Comparison of the Exact Solution and the FEM Solution for 4 elements

N	Exact	FEM	% Error
0	0.050000	0.050000	0.0000
1000	0.123494	0.123494	0.0000
2000	0.196988	0.196988	0.0000
3000	0.270482	0.270482	0.0000
4000	0.343976	0.343976	0.0000

Table 2: Comparison of the Exact Solution and the FEM Solution for 10 elements

Cycle	Crack_FEM	Crack_EXACT
0	0.0500000000	0.0500000000
400	0.0793976197	0.0793976197
800	0.1087952393	0.1087952393
1200	0.1381928590	0.1381928590
1600	0.1675904787	0.1675904787
2000	0.1969880983	0.1969880983
2400	0.2263857180	0.2263857180
2800	0.2557833376	0.2557833376
3200	0.2851809573	0.2851809573
3600	0.3145785770	0.3145785770
4000	0.3439761966	0.3439761966

In this paper, the problem being analyse is the one that involves crack growth from one edge of a plate. The plate is made up of Al 2024 - T351 alloy.

In the analysis, the Priddle crack growth model was adopted, and the finite element method was used to discretize the entire domain of the plate. The domain was discretized into four linear elements. In other to analyse these elements, a linear interpolation function was used.

The graph of crack growth length was plotted against the number of cycles. The number of cycles were between 0 and 4000. This was shown in Fig. 1 for the finite element method and the exact differential equation method. It was observed that as the number of cycles increases, the crack length increases as well. This shows that there is a direct relationship between the number of cycles and the crack growth. The slope of the graph will give us idea of the crack growth rate of the material under consideration. The slope of the graph was estimates to be 7.3494×10^{-5} which represent 'y' from the governing equation. This means that the crack growth rate is dependent on the material properties.

In the cause of the analysis, there was an initial crack length of 0.05mm. This initial crack length of the material represents the intercept of the graph as shown in Fig. 1 also. Subsequently, as the number of cycles increases, the crack growth also increases but at this point in time linearly. As the number of cycles increases, the crack growth rate increases. At this time, the crack growth rate is coming close to the critical stage.

To verify the accuracy of the results obtained from the finite element method, the same problem was solved using the exact differential equation method. The results obtained from the finite element method were compared with the results obtained from the exact differential equation method. It was observed from the two methods that their results were in good consonance with one another. From the results shown in Table 1, even with just four linear element, we were able to have a very high accuracy. Any effort of trying to increase the number of elements will seem like reinventing the wheel. This was shown in Table 2 for 10 elements. The advantage of the finite element method over the exact differential equation method is that the FEM gives results that represent the different nodes for the whole material under consideration at the same time unlike the result from the exact differential equation method that provide discrete result at a time and need further iteration to determine the values at other points of the plate.

Conclusion: So far, the finite element method has been used to obtain the fatigue crack growth in an aluminium alloy material (Al 2024 – T351). The results obtained from the FEM were compared with the results obtained from the exact differential equation method and it was discovered that both results agrees. The result obtained shows that the finite element method is an efficient and accurate method for analysing engineering problems including those involving fluid mechanics.

REFERENCES

Abhishek, K; Rama, CM; Nagesh, RI (2013). A Study of the Stress Ratio Effects on Fatigue Crack Growth using LOWESS Regression. *Proc. of the Intl. Conf. on Advances in Civil, Structural and Mechanical Engineering –CSM*. pp. 47-51

Broek, D (1989). The Practical Use of Fracture Mechanics, Kluwer Academic Publishers.

Camacho, GT Ortiz, M (1996). Computational modelling of impact damage in brittle materials", *Int. J. Solids Structures*, 33, pp. 2899-2938.

Camacho, GT; Ortiz, M (1997). Adaptive Lagrangian modelling of ballistic penetration of metallic targets. *Comput. Meth. Appl. Mech. Eng.,* 142, 269-301.

Collipriest, JE (1972). In: "An experimentalist's view of the surface flaw problem." New York: ASME; p. 43–61.

Forman, RG (1972). "Study of fatigue crack initiation from flaws using fracture mechanics theory," *Eng. Fract. Mech*.

Newman Jr JC (1981). A crack closure model for predicting fatigue crack growth under aircraft spectrum loading. In: Chang JB, Hudson CM, editors. Methods and models for predicting fatigue crack growth under random loading. ASTM STP 748, p. 53–84.

Paris, PC; Erdogan, F (1963). "A critical analysis of crack propagation laws" *J. of B. Eng., Trans, ASME, Series D*, 85, pp.528-534.

Schijve, J (1999). The significance of fractography for investigations of fatigue crack growth under variable-amplitude loading. *Fatigue Frac. Eng. Mater Struct.* 22:87–99.

Schutz, W (1989). Standardized stress-time histories—an overview. In: Potter JM, Watanabe RT, editors. Development of fatigue loading spectra. ASTM STP 1006, p.3–16.

Walker, EK (1970). "The effect of stress ratio during crack propagation and fatigue for 2024-T3 and 7076-T6 aluminium. In: Effect of environment and complex load history on fatigue life", ASTM STP 462. pp. 1–14.

Weertman, J (1966). "Rate of Growth of Fatigue Cracks Calculated from the Theory of Infinitesimal Dislocations Distributed on Plane," *Int. J. of Fract. Mech.* 2: 460-467.

Wu, A; Ma, NX; Murakawa, H; Ueda, Y (1996). Effects of Welding Procedures on Residual Stresses in T-Joints. *JWRI,* 25 (4) 81-89.

Wu, J; Ellyin, F (1996). A Study of Fatigue Crack Closure by Elastic-Plastic Finite Element Analysis for Constant-Amplitude Loading. *Inter. J. Frac.* 82, 43-65.